



Envisioning faults beyond the framework of fracture mechanics

Anita Torabi^{a,*}, John Rudnicki^b, Behzad Alaei^{a,c}, Giuseppe Buscarnera^b

^a Department of Geosciences, University of Oslo, postboks 1047, Blindern 0316, Oslo, Norway

^b Department of Civil and environmental engineering, Northwestern University, 2145 Sheridan Road, Tech A333, Evanston, IL 60208, USA

^c Earth Science Analytics, Strandveien 37, 1366 Lysaker, Norway

ARTICLE INFO

Keywords:

Fault
Fracture mechanics
Earthquake rupture
Seismic data
Seismology
Statistical law

ABSTRACT

Faults are complex structures that substantially influence the mechanical behavior and hydraulic connectivity of rock formations. Therefore, studying faults is important for a variety of disciplines such as geoscience, civil, geotechnical, reservoir engineering, and material science among others. Researchers from these disciplines have considered different aspects of faults, namely geometry, petrophysical properties and mechanics. Until now, these studies have evolved separately and at different scales, making it difficult to connect the geometric development of fault structure to its mechanics. The current understanding of fault geometry and growth is based on fracture mechanics and on many qualitative and quantitative studies on outcrop and seismic reflection surveys among other datasets. The application of fracture mechanics theory is mostly confined to simple geometries: elliptical models for a single fault plane and uniform properties. These applications predict the maximum displacement at the center of the fault, which is not in agreement with the new findings from 3D seismic and outcrop studies. These fracture mechanics models emphasize fault propagation along strike (in 2D). Although they can include the presence of a process zone at the fault tip, the models fail to explain the development of cross-fault damage zones and localization within the fault core as well as fault segmentation and displacement partitioning. Therefore, it is timely to revise the existing applications of fracture mechanics to simple fault geometries and to develop a data-driven fault mechanics possessing closer agreement with real, observed subsurface heterogeneity. This would allow better prediction of fault geometry, propagation, and growth in 3D. We suggest recent advances in non-destructive numerical characterization of faults and application of Deep Neural Networks (DNN) to map fault geometry and predict its properties from seismic data enable us for the first time to extract simultaneously faults' geometrical and mechanical properties at an unprecedented speed and accuracy, thus resolving the 3D fault shape and properties in ways that were unthinkable just a decade ago.

1. Introduction

Faults are complex structures, which introduce heterogeneities and anisotropic properties to their host rock. Understanding fault geometry (Fig. 1a), petrophysical and mechanical properties, and processes of faulting are important research areas for many applications such as earthquake seismology and geological hazard studies (Martel and Pollard, 1989; Bayart et al., 2015; Klinger et al., 2018; Kearsse and Kaneko, 2020); geothermal energy managements (Loveless et al., 2014); waste disposal, hydrogen and CO₂ storage underground (Rohmer et al., 2015); petroleum exploration and production (Gabrielsen et al., 1990; Fisher and Knipe, 2001); hydrogeology (Bense et al., 2013); civil and structural engineering (Katsanos et al., 2010), geotechnical and mining

engineering (Wang et al., 2016), and material science (Hutchings and Shipway, 2017).

Researchers from a variety of disciplines have considered different aspects of fault geometry, properties and mechanics. However, these studies have evolved separately and at different scales, making it difficult to connect the geometric development of fault structure to its mechanics. Experimental and theoretical studies concerning strain localization in rocks in the form of faults and fractures are usually at small scale and suitable to model the initiation and onset of the localization process of deformation but not the propagation and growth of faults (Bésuelle and Rudnicki, 2004; Di Toro et al., 2006; Torabi et al., 2007; Doan and Gary, 2009; Alikarami et al., 2014; Skurtveit et al., 2013; Bayart et al., 2015; McBeck et al., 2022). Seismological studies are

* Corresponding author.

E-mail addresses: anita.torabi@geo.uio.no (A. Torabi), jwru@northwestern.edu (J. Rudnicki), behzad.alaei@earthanalytics.no (B. Alaei), g-buscarnera@northwestern.edu (G. Buscarnera).

<https://doi.org/10.1016/j.earscrev.2023.104358>

Received 25 October 2022; Received in revised form 22 January 2023; Accepted 9 February 2023

Available online 13 February 2023

0012-8252/© 2023 The Author(s). Published by Elsevier B.V. This is an open access article under the CC BY license (<http://creativecommons.org/licenses/by/4.0/>).

yet to include realistic complex fault structures in their models, although in recent years, some studies have moved to this direction (e.g. Klinger et al., 2018; Romanet et al., 2018; Okubo et al., 2019).

The current mechanical models of faulting used to predict fault geometry and propagation are limited to the applications mentioned above and originate mostly from fracture mechanics theories (Cowie and Scholz, 1992; Rice, 1968; Palmer and Rice, 1973; Rudnicki, 1980) that are applied on restricted simple geometries of faults. Inaccessibility to 3D fault structure and bias in the fault datasets, make it hard to develop and test more complex fault mechanical models.

In structural geology, a fault is usually identified by a principal fault plane (main slip surface) and its surrounding architectural components, fault core and damage zone (Caine et al., 1996; Torabi and Berg, 2011; Fig. 1a). Fault damage zone may include minor faults, drag folds, fractures or deformation bands depending on the initial porosity of host rock (Torabi et al., 2020). Fault core includes higher strained features than damage zone and involves fault gouge, strained lenses of host rock and diagenetic features and sometimes clay smear (Braathen et al., 2009; Torabi et al., 2019b). Fault geometric attributes are displacement, length, height, number of fault segments (Fig. 1a, Cowie and Scholz, 1992; Torabi and Berg, 2011; Torabi et al., 2019a), fault core thickness and damage zone width around the fault plane (Fig. 1a, Caine et al., 1996, Childs et al., 2009; Choi et al., 2016; De Rosa et al., 2018; Torabi et al., 2019b). These geometric attributes have been used to characterize the fault geometry and predict the fault growth and mechanics through fault scaling laws (Fig. 1b).

The fault geometric data are principally derived from different sources such as outcrop geology, earthquake statistics, reflection seismic data, well data, and satellite imagery (Camanni et al., 2019; Delogkos et al., 2020; Roche et al., 2021; Antoine et al., 2022). However, depending on the resolution of the measuring methods and the fault accessibility, fault geometric characteristics could be constrained and biased (Torabi and Berg, 2011). The fault plane 3D shape is usually reconstructed from interpretation of 2D horizontal and vertical sections of seismic and outcrop data. Lateral and vertical segmentations in 3D affect both fault length and displacement (Roche et al., 2021) but because of the limitation of the methods used to study faults, this effect has not been sufficiently acknowledged for a single (a fault with its internal segments) as well as interacting neighboring fault planes. Details of fault damage zone and core could be mainly studied in 1D, 2D, or more recently 2.5D datasets from outcrops (Torabi et al., 2020; Torabi et al., 2019b; and Delogkos et al., 2020). A fault can change its orientation, type, and kinematics; however, these changes cannot be truly captured through 1D or 2D measurements of a fault. Based on the

current state of the art and considering different disciplines, we have identified several challenges related to the fault studies in understanding fault mechanics: (i) inaccessibility to fault 3D structure; (ii) low resolution images of subsurface faults; (iii) method-related constraints and uncertainties; (iv) lack of sufficient fault data from different scales; (v) mixing data of different origins e.g. seismically active faults with non-active faults, *syn*-sedimentary faults with post-sedimentary faults; (vi) neglecting the effect of pre-existing geological structures; (vii) non-integration of fault geometric and mechanical properties; (viii) overly idealized mechanical models of fault structures.

In this contribution, we address the current state of the art on fault geometry and architecture (section 2); earthquake ruptures (section 3), fault scaling laws (section 4), and numerical modeling (section 5) in light of these challenges and discuss them with regard to fracture mechanics limitations. Our main objective is to introduce a new interdisciplinary vision of fault mechanics by providing a critical view on present fault growth and statistical models in order to bridge the gaps between different disciplines and feed the future research direction on this topic. We argue that simple fracture mechanics models are not adequate to describe the complexity of fault systems revealed by recent observations. At a minimum, models which go beyond simple shapes (circular or elliptical) with uniform frictional resistance and small cohesive zones at the fault tip are needed. These will require numerical calculations. Currently, with the new and improved fault 3D data available through application of seismic attributes and machine learning on seismic data (e.g. Torabi et al., 2019a, Roche et al., 2021; Michie et al., 2021; Torabi and Alaei, 2022), and detailed observations of faults in outcrops using advanced imaging techniques such as lidar and satellite imagery (Helton et al., 2022; Marple et al., 2020; Petricca et al., 2021) the development of more complex fault models would be needed in the future.

Recent advances in non-destructive numerical characterization of faults (e.g. Shahin et al., 2021) and application of Deep Neural Networks (DNN) to map fault geometry (e.g. Ahmed, 2021; Michie et al., 2021; Bönke, 2022; Torabi and Alaei, 2022) and predict its properties from seismic data (e.g. Wu et al., 2021; Torabi and Alaei, 2022) enable us for the first time to extract simultaneously faults geometrical and mechanical properties at an unprecedented speed and accuracy, thus resolving the 3D fault shape and properties in ways that were unthinkable just a decade ago. In this regard, we have carried out a pilot test on large normal faults from the Norwegian North Sea using high quality 3D seismic and well data with good coverage and quality. Utilizing DNN, we extracted and integrated the geometry and a mechanical property (Poisson's ratio) of faults in order to better constrain the fault 3D

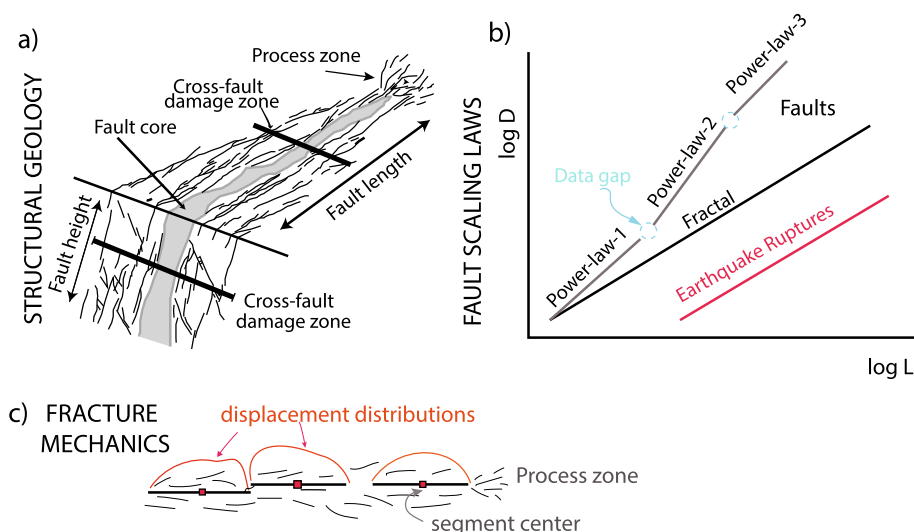


Fig. 1. a) Schematic illustration of a fault showing fault plane geometric attributes such as fault length and height as well as fault architectural components including fault core and cross-fault damage zones and process zone (modified after Torabi et al., 2020). b) D-L (displacement-length) as an example of fault scaling laws, for faults of different sizes and earthquake ruptures based on the state-of-the-art. c) Propagating fault segments in 2D based on the current understanding from fracture mechanics.

structure. We argue that these advances can be the cornerstone of a comprehensive revisit of fault mechanics theories in order to cover fault complexity and growth process respecting its size and the level of maturity.

2. Fault geometry and fracture mechanics

2.1. Fault plane geometry

Consistent with fracture mechanics theories, faults are described as having circular tip lines in homogeneous layers with a cone-shape

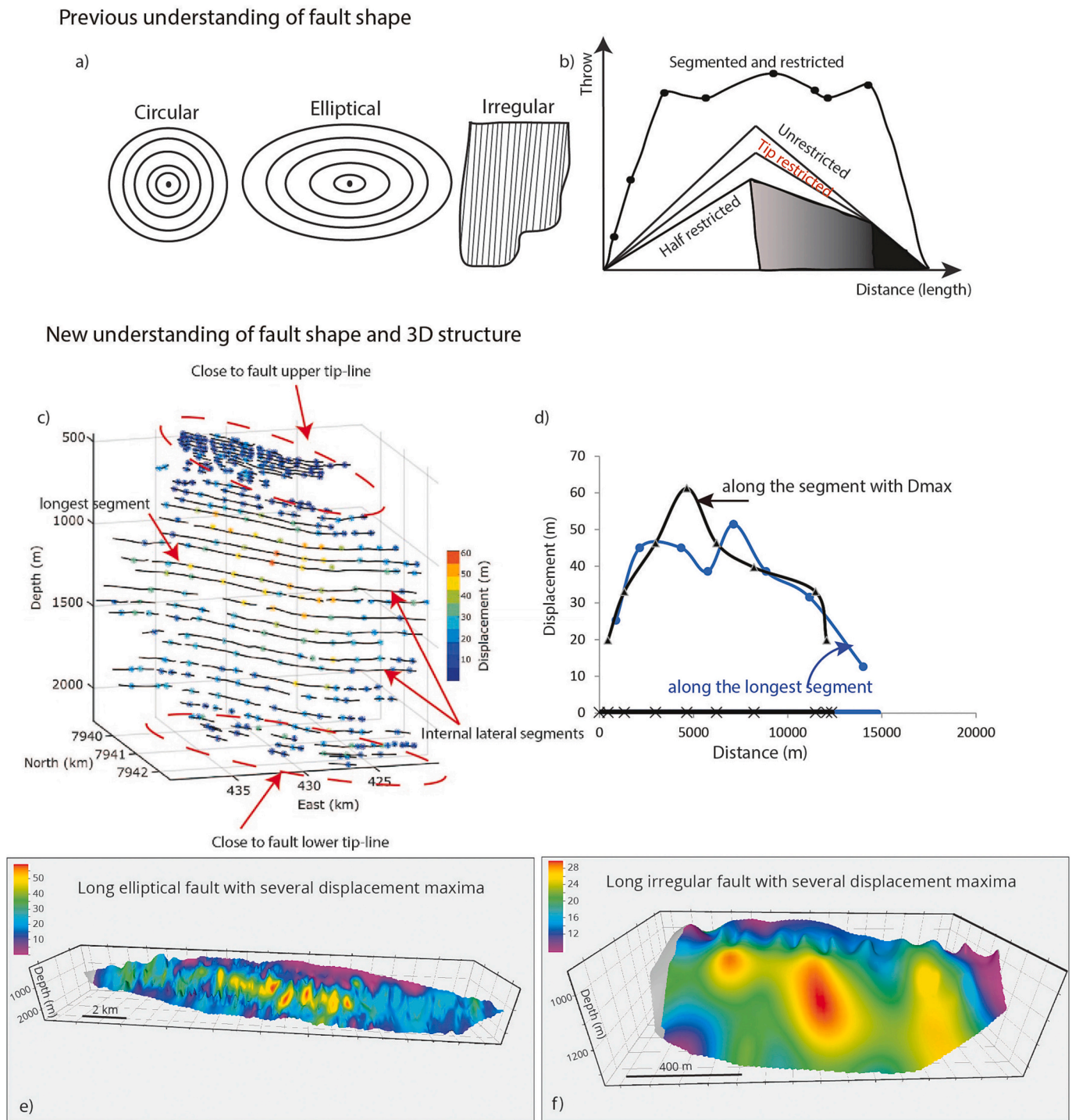


Fig. 2. a) Fault plane shapes based on previous studies as explained in the text; note that maximum displacement is located in the center of fault plane circular and elliptical shapes. b) Throw distribution along fault length based on the previous studies showing cone-shapes and M-shape. c) Internal segments of a fault at different depths directly extracted from seismic data using seismic attributes. The dots with different colors indicate displacement measurements on each fault segment. d) Displacement distribution with irregular and asymmetric shapes along two main segments of the fault within the fault 3D structure as extracted from seismic in c. Note that the maximum displacement is not located on the longest segment. e) Displacement map (in meters) draped on 3D geometry of a fault obtained from 3D seismic data showing semi-elliptical shape, f) Displacement map (in meters) draped on 3D geometry of a fault obtained from 3D seismic data showing rectangular shape. Modified after Torabi et al. (2019a).

displacement (throw) distribution (Figs. 2a and b) and elliptical tip lines when crossing layers of different properties and thickness with a M-shape throw distribution in segmented faults (Figs. 2a and b, Barnett et al., 1987; Nicol et al., 1996; Torabi et al., 2019a). Maximum displacement occurs at the center of an isolated fault that has no interaction with any other surfaces (Figs. 2a and b). These simple fault shapes are currently used for modeling faults and predicting their behavior in the subsurface (Harris et al., 2003; Di Carli et al., 2010; Madariaga and Ruiz, 2016; Treffeisen and Henk, 2020). Utilizing 3D seismic data, Marchal et al. (2003) suggested an irregular fault plane with several bifurcated tip lines (Fig. 2a).

Recent results using direct fault imaging on forty 3D seismic surveys from the Barents Sea indicate that the long faults with maximum length or $L_{max} > 1000$ m can have a variety of shapes such as irregular, elliptical, and rectangular (Fig. 2e and f), while medium size faults $1 \leq L_{max} \leq 1000$ m have irregular shapes (Torabi et al., 2019a). In addition, Torabi et al. (2019a) found a large aspect ratio (maximum length/height is up to 16) for these faults and that the maximum displacement for a single fault could be located anywhere in the 3D structure of a fault and not necessarily in its center (Table 1 in Torabi et al., 2019a). The displacement data measured on individual segments of faults of different sizes (at different depths, Figs. 2c, and d) shows no similarity to the current models presented in Figs. 2a and b (Torabi et al., 2019a). This is a very important data driven finding that encourages delving more into the link between fault geometry and mechanics. This implies that the fault plane resistance (friction) is not uniform, which could be caused by the fault internal segmentation (Roche et al., 2021) or the interaction with any other (neighboring) fault or free surfaces.

2.2. Fault architectural components

The simplest fracture mechanics models such as the Linear Elastic Fracture Mechanics criteria (LEFM) (Griffith Criterion, e.g. Rice, 1968) used to explain fault growth assume that faults are shear fractures with uniform friction, propagating at their tips (Fig. 1c). Although LEFM predicts a stress singularity at the fault tip, it is a good model when any inelastic behavior occurs in a region with a length scale smaller than any other in the problem. Propagation of the fault is predicted to occur when the coefficient of that singularity (stress intensity factor) reaches a critical value (or, equivalently, that the energy released by an increment of growth reaches a critical value). Cohesive zone models (Barenblatt, 1959, 1962, Palmer and Rice, 1973; Rudnicki, 1980) take explicit account of inelastic behavior in a narrow zone extending from the fault tip. When the length of this zone is small compared to other length scales in the problem, the cohesive zone model is equivalent to LEFM but provides an interpretation of the critical stress intensity factor or energy release rate. If the cohesive zone is not small, the model departs from LEFM. Although cohesive zone models are an improvement in taking account of inelastic processes at the tip, they are restricted to narrow regions ahead of the tip. More generally, models need to account for inelastic deformation or the presence of small faults and fractures off of the main fault plane.

Experimental studies of shear fracture propagation (Moore and Lockner, 1995) confirm inelastic deformation around the fracture tip, where the fault forms by breaking through the process zone after a critical crack density happens in the fracture tip. Geological observations confirm the presence of a process zone or cohesive zone (Perrin et al., 2016) usually with fan shape off-fault splays at the fault tip, which encompasses both tensile fractures and minor fault segments based on outcrop and seismic studies (e.g. Vermilye and Scholz, 1998; Kim et al., 2004; Perrin et al., 2016; Alaei and Torabi, 2017). However, in geology, the damage zone is also laterally classified into cross-fault damage zones along fault length and height (Torabi et al., 2020, Fig. 1a) in addition to around the fault tip damage zone (process zone), which can be a complex product of fault segments and relay zones (Camanni et al., 2021). The physical source and mechanism for cross-fault damage zones with

distributed deformation and minor fault segments in 3D (both along the fault length and height in Fig. 1a) is not explained by present fracture mechanics theories.

Theoretically, when the crack density reaches a critical point of saturation at the fault tip, a fault gouge forms as part of fault core, where eventually the fault center/core (main slip surface or fault plane) would be located (in 2D). With further fault propagation and increasing the displacement at fault center, the fault gouge (core) thickness increases at the center, while the width of the process zone increases at the fault tip (Cowie and Scholz, 1992). However, currently there is no geological data to support these theories for faults and to indicate how the process zone can contribute to the development of cross-fault damage zones.

3. Earthquake ruptures

Faults and earthquake ruptures are two inseparable parts of the same system (Fig. 1c). The characteristics of ruptures are dictated and influenced by the fault structural maturity and complexity as strain is accumulated (Wechsler et al., 2010; Perrin et al., 2015). Regional stress configuration, fault geometry and its preexisting deformation patterns, and orientation of ruptures affect the on- and off-fault damage during earthquakes, which can create complex patterns of ruptures with involvement of new and pre-existing fault segments (Vallage et al., 2016; Klinger et al., 2018). Hence, studying the geometry and mechanisms of the initiation and growth of ruptures and faults, would be mutually beneficial to understand the fault structural complexity.

Distinguishing between the seismic and aseismic (identified by cumulative long-term slip) parts of fault growth in the exhumed and subsurface faults is still challenging and under research despite the new advances in image correlation to study earthquake ruptures on optical satellite images (Klinger et al., 2006; Vallage et al., 2016; Klinger et al., 2018). Recent findings from InSAR (Interferometric Synthetic Aperture Radar) data on active faults provide even more valuable information on the size and shape of the epicentral area, which changes with the type of faulting in different tectonic settings (Petricca et al., 2021). Much of the current research on seismicity of faults has focused on the dynamics and mechanics of earthquake ruptures in order to better predict the future earthquakes (e.g. Aben et al., 2020; Brantut, 2020; Petricca et al., 2021; Antoine et al., 2022; Ulrich et al., 2022; Zaccagnino et al., 2022). This is due to the importance of this topic for its societal and economic impacts.

Seismic moment or M_0 is a linear measure of an earthquake that is measured from seismic radiation or geodetic data (Lay and Wallace, 1995) and has the following relationship with slip, $\Delta\bar{u}$, area of the rupture, A , and shear modulus of rocks, μ .

$$M_0 = \mu \Delta\bar{u} A \quad (1)$$

The rupture area is estimated by inversion of seismic or geodetic data, aftershock area, corner frequency of body wave spectrum, rupture length and therefore the characteristic length scale of the rupture or \bar{L} could be estimated as $A^{1/2}$. $\Delta\bar{u}$ is usually estimated from M_0 and A , although it can also be estimated from the correlation of satellite images before and after the earthquakes with some associated errors (Klinger et al., 2006; Petricca et al., 2021). In seismology, there is discrepancy between the estimated and observed length of ruptures due to uncertainties related to the fault models, inversion techniques for the recorded earthquake data and the measuring methods (Manighetti et al., 2007).

Compiled slip data from earthquake ruptures (both from surface and depth using inversion), and mature faults with accumulated slip (for any fault kinematic type), fit an asymmetric triangular distribution (Manighetti et al., 2005) rather than a cone-shaped symmetrical distribution as suggested by theoretical fault models (Figs. 2a and b) inspired by fracture mechanics (Barnett et al., 1987; Nicol et al., 1996). This observation suggests that the rupture might nucleate wherever the rock strength is low, for example, in the intersection between fault segments

or where the pre-stress on the fault is high (Manighetti et al., 2005), Fig. 1c. Further, the slip asymmetry on ruptures could be influenced by the fault plane roughness and geometry, and the evolution of the off-fault damage zone or process zone (Perrin et al., 2016). The gradient of slip data tapers off toward the rupture tips or where the ruptures reach barriers (Manighetti et al., 2005).

The final parameter that is calculated from all measured or estimated parameters of an earthquake rupture mentioned above is stress drop $\Delta\sigma_s$ that is related to strain drop, where C is a geometric constant of order one.

$$\Delta\sigma_s = CM_0A^{-3} = CM_0L^{-3} \quad (2)$$

Analysis of dynamic rupture models imply that the rupture slip and velocity are linearly scaled with the dynamic stress drop, which is the most important scaling parameter in earthquakes (Scholz, 2019). The stress drop is considered constant within a method but in fact can change over several orders of magnitudes (Allmann and Shearer, 2009) because it is an average over a region of fault obtained from inversions with integral average values (Scholz, 2019). Another issue is that thermal weakening during earthquakes might be associated with an increase in stress drop. These contradict the previous assumption that the stress drop of an earthquake is scale invariant.

Despite the general acceptance of a self-similar or fractal behavior for faults and earthquake ruptures, stress drop varies along ruptures of different size, revealing the importance of heterogeneities, and pre-existing fault structures (fault segments and their interaction) at the time of rupturing (Manighetti et al., 2007). Therefore, through a parameterization approach and statistical model fitting, Manighetti et al. (2007) suggested differentiating between small (young) and mature faults that produce shorter and longer ruptures, respectively, when dealing with seismic hazard studies and scaling laws. In addition, comparison of the scaling relation between seismic moment and rupture length as well as between seismic moment and seismic source duration reveals different scaling laws for small and large (mature) earthquakes both in crustal and oceanic (subduction zones) faults (Denolle and Shearer, 2016). Furthermore, a new study by Zaccagnino et al. (2022) shows that the type of fault and tectonic setting affect the scaling laws of earthquakes (Gutenberg-Richter and Omori laws), meaning that normal faults in extensional regimes create smaller (both in term of magnitude and length of event or L) and more frequent seismic events than reverse and strike slip faults. This might imply that the type of fault and tectonic setting, the width of seismogenic layer in addition to the fault heterogeneities, off-fault damage zone, segmentation, and presence of asperities play an important role in the propagation of ruptures and hence their scaling laws. This would affect the aspect ratio of rupture length and width (height), and therefore influences the seismic moment that is proportional to these two parameters (Scholz, 2019).

4. Utilizing scaling laws to predict fault geometry and growth process

Commonly, fault theoretical and numerical models are based on the assumption that faults are planar, granular, and fractal (scale-invariant) phenomena (Ben-Zion and Sammis, 2003). These assumptions are used to explain the geometric-mechanical-mathematical essence of faults (Fung, 1977; Ben-Zion and Sammis, 2003). On one hand, mature (large displacement) faults are considered planar zones in a continuum solid that have been localized due to strain softening. On the other hand, smaller faults or distributed damage around the mature faults are related to strain hardening process resulting in granulation of rocks. However, the strain softening and hardening processes might work interchangeably during the entire faulting process, depending on the slip rate. Despite these two different views for mature and small faults, the process of faulting (including the earthquake ruptures) and distributions of faults and ruptures' geometric data are considered fractal and scale-

invariant (Ben-Zion and Sammis, 2003; Manighetti et al., 2005) repeating themselves at different scales, Fig. 1b.

In the last two decades, structural geologists working on normal faults in extensional systems (mainly *syn*-sedimentary faults through growth strata) have suggested two models of fault growth, an isolated and a coherent fault model (Rotevatn et al., 2019). The isolated fault model (e.g., Walsh et al., 2003; Cowie et al., 2000) better explains the propagation at fault tip and fits the fractal concept of fault growth, by predicting a mutual increase in fault length and displacement similar to the prediction by the fracture mechanics. Conversely, the coherent fault model considers the fault segments as a coherent part of the fault from the initial stage toward a mature fault, causing a constant fault length while accommodating displacement (e.g., Walsh et al., 2002; Giba et al., 2012). This could also be described by a simple fracture mechanics model with pinned ends and increasing loading stress. However, recent studies show that the fault growth mechanism could change over the time and with respect to the underlying structures and therefore a combination of these two models could better explain the fault growth at different stages and scales (Rotevatn et al., 2019; Torabi et al., 2019a; Bramham et al., 2021).

Despite the uncertainty in geological conceptual models on how and when cross-fault and tip-damage zones (process zone) form, fault damage zone development (damage zone width, W) is directly correlated with fault displacement ($D - W$ scaling-law) in order to predict the fault growth at different scales (Beach et al., 1999; Shipton et al., 2006; Savage and Brodsky, 2011; Torabi and Berg, 2011).

Furthermore, the scaling relationships between fault displacement, D , and other fault geometric attributes such as length (L), (e.g. Cowie and Scholz, 1992; Kim and Sanderson, 2005; Torabi et al., 2019a) and fault core thickness, T and spacing of the fault segments (Childs et al., 2009) have been used to predict the fault geometry, growth and evolution and to explain the faulting process by fracture mechanics (Scholz, 2007).

In addition, fault scaling laws are used to populate faults in geological models in order to simulate subsurface reservoirs (Harris et al., 2003). This is despite the fact that there are still uncertainties in the measured fault geometric attributes, the fault 3D shape and displacement distribution, as well as in constraining the extent of fault core and damage zone.

Most of the fracture mechanics theories including LEFM (Eq. 3), result in a linear scaling law (fractal) between D_{max} and L , where $\Delta\sigma$ is the stress drop, ν is Poisson's ratio, μ is friction with assuming an elliptical D distribution (Scholz, 2007).

$$D_{max} = \Delta\sigma \frac{2(1 - \nu)}{\mu} L \quad (3)$$

This is consistent with the scaling law suggested for D - L relation (Eq. 4) in most geological literature (e.g. Cowie and Scholz, 1992, 2007; Schultz and Fossen, 2002; Kim and Sanderson, 2005; Scholz, 2007), where $n = 1$ and only γ (intercept with the Y -axis) can change depending on the lithology, tectonic setting and depth of faulting.

$$D = \gamma L^n \quad (4)$$

Walsh and Watterson (1988); Marrett and Allmendinger (1991) reported higher values than 1 for n , whereas, Cowie and Scholz (1992) argue that by mixing of data of different sources, the previous studies concluded higher n values than 1. They further claimed that separating data based on lithology and tectonic setting, only affects γ and the power-law exponent remains constant equal to one (Cowie and Scholz, 1992). For values of $n > 1$, the stress drop has to increase with fault length and therefore the fault cannot grow in length (Scholz, 2007). Manighetti et al. (2007) argue that the stress drop and the width of rupture is influenced by the maturity of fault and its pre-existing structures (including asperities), therefore affecting the rupture length and the scaling law between D and L .

However, detailed analysis of a compilation of all available fault and

rupture datasets and separating data based on rock type and tectonic setting in a review study by Torabi and Berg (2011), shows that there is no global scale-invariant or fractal relationship between fault geometric attributes. In contrast to the previous studies, this study further indicates that the power-law exponent in $D - L$, $D - T$, $D - W$ can in fact change with the size and maturity of fault. Utilizing advanced statistical analysis on the same datasets in Torabi and Berg (2011) and acknowledging the effect of lithology and type of faulting, Kolyukhin and Torabi (2012) suggested a two-slope power-law relation for scaling of fault displacement versus other fault geometric attributes, where in some cases $n > 2$. This finding is inconsistent with the fractal view of faults. In addition, Kolyukhin and Torabi (2013) suggested that truncated power laws better fit to the univariate geometric fault data such as fault length, reflecting the importance of the size and maturity of fault. This is inconsistent with the previous studies that suggested power-law univariate distributions for smaller faults (involving low strain) and exponential distribution for larger faults (involving high strain) (Scholz and Cowie, 1990).

5. Fault numerical models and fracture mechanics

While modern sensing enables us to characterize the 3D structure of faults in ways that were unthinkable a few decades ago, the formulation of geomechanical models able to harness such extensive data streams is increasingly becoming an essential element to explain the history of faults and predict their current and future functioning mechanisms.

Rock friction has traditionally been described as stick-slip, but observations by (Dieterich, 1979; Ruina, 1983) nearly 40 years ago and subsequently by many others (e.g. Marone et al., 1990) have shown that rate and state friction is a more robust description. In this formulation, the coefficient of friction depends on the velocity of sliding and one or more state parameters that characterize the evolution of the sliding surface. This description incorporates healing of asperity contacts and, consequently, can exhibit repeated events and both stable (slow, aseismic) and unstable (rapid, seismic) slip. Implementation of these into models of earthquake ruptures has motivated the development of boundary integral methods for dynamic ruptures (Day et al., 2005; Kaneko et al., 2008; Lapusta and Liu, 2009). Simulations have illuminated the conditions for many kinds of earthquake behavior, e.g. whether slip is crack-like or pulse-like (Liu, 2009). Recent theoretical and numerical works have addressed the crack-like behavior of frictional slip along the earthquake ruptures through some modification to the fracture mechanics energy balance equations. The main suggested modification is the deviation related to non-edge-localized dissipation, which highlights the importance of the residual shear strength along the ruptures (Barras et al., 2019; Brener and Bouchbinder, 2021).

Numerical studies of active faults that are affected by slow slip, creep and seismic rupturing show the importance of fault complex geometry including the fault segmentation and roughness in the interplay between the three above-mentioned mechanisms, and the need for more advanced models beyond simple elastic models to include viscoelasticity (Romanet et al., 2018; Shahin et al., 2021). Furthermore, numerical works on earthquakes using visco-elasto-plastic layers subjected to an invariant rate-and-state-dependent friction and inspired by fault outcrop data and experiments reveal the importance of including both dynamic earthquake ruptures and aseismic deformation contributing to localized deformation and the evolution of fault damage zone (Preuss et al., 2020). In addition to local stress changes, the fault interactions between different segments was found to be one of the main contributors to the dynamic changes in the fault geometry and orientation, which is progressively optimized (Preuss et al., 2020).

In this context, the integration of established interpretation frameworks based on fracture mechanics with advances in the modeling of rock inelasticity is one of the primary challenges. In particular, few methods currently recognize that the deformation of rocks in the vicinity of an advancing fault tips possesses non-negligible viscoplastic

components, able to dissipate the elastic stored energy through both homogeneous and inhomogeneous deformation (Rudnicki and Rice, 1975; Buscarnera and Laverack, 2014; Shahin et al., 2021). Given the complexity and lack of symmetry of the stress field around the tip of shear fractures, this attribute is likely to play a key role in explaining the complex geometry of faults disclosed by subsurface structural mapping on seismic data. Most importantly, disclosing the impact of near-tip rock inelasticity is likely to play a crucial role to examine the role of pore fluids on the dynamics of fault growth. In fact, the transition from dilatative to contractive inelastic regimes, combined with the stress-path dependence of near-fault materials, can be expected to alter the pressure conditions of subsurface fluids by creating short-lived pressure pulses which may expand the size of the inelastic zone in front of a fault, thus influencing its shape and rate of growth (Garagash and Rudnicki, 2003).

Another open question that can benefit from the synergistic use of geomechanical modeling and subsurface characterization is the analysis of frictional constraints behind fault tips. In fact, frictional slip and fault growth are inextricably coupled, thus requiring development and use of computational models equipped with interface laws able to capture the heterogeneous shear mechanisms controlled by the competition between volume change in the fault gouge and asperity damage (Marone et al., 1990).

Future integration between high-resolution 3D fault characterization and geomechanics will also require numerical models able to effectively simulate advancing fault zones. In fact, as shear fractures progress, they will leave a damaged zone behind the tip that depends on the parameters of the inelastic deformation. Resolving this complex process requires sophisticated numerical tools, such as Extended Finite Element Methods (Moës et al., 1999), as well as suitable slip localization and growth criteria embedded into the finite elements.

Although finite element methods can be used, boundary element methods (Cruse, 1998; Cheng and Cheng, 2005), dislocation solutions (Jeyakumaran et al., 1992; Wu et al., 1990) or methods based on integral equations (Viesca and Garagash, 2018) are more efficient because they require discretizing only crack surfaces or boundaries.

Models with these features may enable unbiased simulations of fault growth patterns, thus elucidating if the initial and evolving stress field around the tip of a propagating fault is sufficient to explain the complex geometry of faults observed in natural settings.

The success of such modeling advances will also depend on our ability to convert complex subsurface architectures into realistic, yet tractable, simulated fault networks. This step can benefit from recent progress in mapping measurements of spatial heterogeneity into numerical replicas of geophysical systems at laboratory scale (Shahin et al., 2020). Such capabilities, however, are still hardly deployed beyond the scale of rock cores. The extensive data streams of subsurface heterogeneity detailed in the previous section (section 2.1), therefore offer unprecedented opportunities to constrain the initial conditions of the 3D numerical models with rich, abundant, spatially heterogeneous data of location, geometry, and intersection between different families of faults in a fault system.

Advancement of the current standards of geomechanical modeling based on the directions outlined in this section have future potential to open the way for improved data-driven simulation strategies enabling the geoscience community to examine the past and current data under a new light, thus setting the stage to move beyond the current simplified geometric/mechanical theories of fault activation, growth and coalescence which often hinder our ability to explain the complexity of nature.

6. Synthesis and future works

Despite great progress in earthquake modeling, simulations have been largely confined to the propagation of planar surfaces. There is a need for efficient numerical methods to address the development of complex fracture systems representative of outcrop and seismic

observations. Although there has been some work in modeling off fault damage (Viesca et al., 2008; Templeton and Rice, 2008; DeDontney et al., 2011) there remains much to be done in this area. Modeling has been confined to inelastic behavior near the fault surface. Recent work (Shahin et al., 2021) has shown that fully nonlinear behavior in the bulk can precipitate the initiation and evolution of localized deformation having features of natural faults. The role of fully non-linear behavior on the development of fault systems is in its early stages.

We suggest that any fault mechanical model in the future should respect the subsurface heterogeneities and fault 3D structure and length scale. The current fault mechanical models should be revised for friction non-uniformity, fault segments, fault shape, and displacement distribution. This means revising the assumptions of planar cracks with uniform friction as well as the simple elliptical geometry of the fault in these models. The revised models should address the importance of fault segmentation, cross-fault damage zone and growth in addition to the propagation at the fault tip. These are very important topics that need higher resolution data from further investigation of faults at different scales through 3D seismic studies, borehole data, outcrop studies using drone and lidar images and in-situ measurements of fault rock properties, as well as gathering data from active faults prior, during and after earthquakes using advanced techniques such as InSAR (e.g. Torabi et al., 2019a, 2020; Torabi et al., 2019b; Brodsky, 2020; Michie et al., 2021; Petricca et al., 2021; Tibaldi et al., 2021; Ybanez et al., 2021).

The challenges described earlier clearly show that integrating data from different scales of both geometry and fault rock properties is one of solutions (if not the only one) to unlock some of the unresolved issues of faulting that we have presented in this paper. Such integration of fault geometry and corresponding fault rock properties will also enable us to fill in the remaining gaps in fault data from different scales, which would improve the fault scaling laws.

New developments in fault imaging and fault rock property prediction (e.g. elastic properties) utilizing DNN on 3D seismic and 1D well data, respectively, would certainly improve and accelerate these studies.

6.1. A pilot study utilizing DNN

Integrating fault geometry and mechanical properties, provide a better constraint on 3D fault structure. As the first study in this direction, we have integrated and correlated fault geometric attributes with fault mechanical properties (e.g. Poisson's ratio) in order to better characterize and constrain the fault structure in 3D. We suggest this could be one of advanced methods allowing us to connect the development of fault geometry and architecture to its mechanical growth (Fig. 3). Our case study involves large faults on 3D seismic data from the Norwegian North Sea. The applied approach has two steps, fault geometric mapping followed by predicting fault rock mechanical properties, both using supervised DNN (Torabi and Alaei, 2022). In our first attempt in this path, we have used EarthNet (Oikonomou et al., 2019) to carry out the two steps study of fault geometry and properties using DNN. For seismic interpretation of faults (step 1) different DNN networks have been tested and combined including light Unet (modified from Ronneberger et al., 2015), efficient Unet (modified from Tan and Le, 2019), and TransUnet (modified from Chen et al., 2021). The training data for this step are labels of faults (versus host rock) and full stack seismic data. Application of different DNN architectures enable us to create final fault probability volumes using ensemble models. For the 3D property prediction of mechanical properties (step 2 of the study) we used Unet++ network (modified from Yang et al., 2020). The training data for this step could be any mechanical properties at well locations derived from wireline logs (as labels) and the same seismic data used for obtaining the geometry at the first step. The seismic data are quality controlled or QCed angle stacks plus background low frequency model. Well tie and upscaling using Backus averaging and window-based methods have been performed prior to model training. Blind testing has been used to verify the quality of the predictions away from the wells in addition to

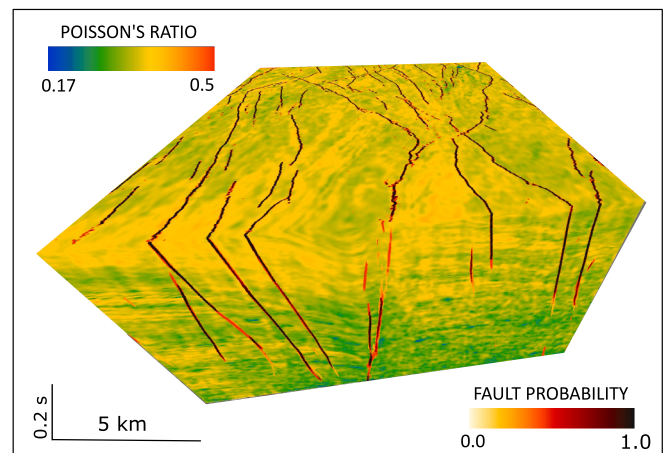


Fig. 3. Combined results from the two-step approach, utilizing DNN to capture the fault geometry (fault traces probability) and fault rock property (Poisson's ratio). The 3D volume is Poisson's ratio distributed around the geometry.

machine learning usual QC (monitoring loss function behavior as well as metrics).

This two steps approach allows us to quantitatively measure the accuracy of the predictions for both fault geometry and fault rock properties. For fault geometry mapping, we generated fault probability volumes out of machine learning fault prediction volumes. An example is given in Fig. 3, where the colors representing faults correspond to different probability. For the step 2 of the approach (seismic scale prediction of fault rock properties e.g. Poisson's ratio in Fig. 3), we addressed the uncertainty by using ensemble approach. This enables us to get predictions and standard deviation at each depth sample. The 3D volumes of mechanical properties derived from our DNN approach will be used to construct different scanlines along and across faults at different depth levels to study the possible effect of faulting on mechanical properties of host rock. In addition, we will link the variations of mechanical properties to certain stratigraphic interfaces (where faults have displaced) by mapping the properties at those stratigraphic levels.

Using the DNN for both fault geometric and fault rock properties prediction, we will be able to generate large amount of data from different tectonic settings (and scale) in a very short time and eliminate some of the uncertainties related to conventional seismic interpretation of faults. Such a database is essential to study mechanical models governing fault growth with a data driven link to their 3D shape in order to overcome the challenges given in the introduction.

This study reveals that not only new data (e.g., 3D fault structure characterization) would enable us to improve the theory, but also advances in fracture or fault mechanics from other domains (e.g., earthquake seismology) can inspire new ways of looking at the data. This is a vision piece stressing that the times are mature to go beyond standard theories based on simple models, but also welcoming new theories that enable us to look at past (and current) data under a new light.

Declaration of Competing Interest

The authors declare that they have no known competing financial interests or personal relationships that could have appeared to influence the work reported in this paper.

Data availability

The authors are unable or have chosen not to specify which data has been used.

Acknowledgements

We acknowledge the Energy office at the University of Oslo. We are grateful to Norwegian Petroleum Directorate (NPD) for providing the seismic and well data through Diskos database. Earth Science Analytics is thanked for granting access to EarthNet to the University of Oslo.

References

- Aben, F.M., Brantut, N., Mitchell, T.M., 2020. Off-Fault damage characterization during and after experimental Quasi-Static and dynamic rupture in crustal rock from laboratory P Wave tomography and microstructures. *J. Geophys. Res. Solid Earth* 125 (8), 2020. <https://doi.org/10.1029/2020jb019860>.
- Ahmed, S., 2021. Structural analysis of Horda Platform and Stord Basin in the Norwegian North Sea using Machine Learning methods. University of Oslo. Master thesis.
- Alaei, B., Torabi, A., 2017. Seismic imaging of fault damage zone and its scaling relation with displacement. *Interpretation* 5, 4, SP83-SP93.
- Alikarami, R., Andò, E., Gkiouas-Kapnisis, M., Torabi, A., Viggiani, G., 2014. Strain localization and grain breakage in sand under shearing at high mean stress: insights from in-situ x-ray tomography. *Acta Geotech.* 10 (1), 15–30. <https://doi.org/10.1007/s11440-014-0364-6>.
- Allmann, B., Shearer, P.T., 2009. Global variations of stress drop for moderate to large earthquakes. *J. Geophys. Res. Solid Earth* 114, B01310. <https://doi.org/10.1029/2008JB005821>.
- Antoine, S.N., Klinger, Y., Delorme, A., Gold, R.D., 2022. Off-Fault Deformation in Regions of complex Fault Geometries: the 2013, Mw7.7, Baluchistan Rupture (Pakistan). *J. Geophys. Res. Solid Earth* 127, 11. <https://doi.org/10.1029/2022JB024480>.
- Barras, F., Aldam, M., Roch, T., Brenner, E.A., Bouchbinder, E., Molinari, J.-F., 2019. The emergence of crack-like behavior of frictional rupture: Edge singularity and energy balance. *Phys. Rev. X* 9, 041043.
- Barenblatt, G.I., 1959. The formation of equilibrium cracks during brittle fracture: general ideas and hypothesis, axially symmetric cracks. *Appl. Math., Mech.* 23, 622–636.
- Barenblatt, G.I., 1962. The mathematical theory of equilibrium cracks in brittle fracture. In: *Advances in Applied Mechanics*, Vol. VII., Academic Press, pp. 55–129.
- Barnett, J.A.M., Mortimer, J., Rippon, J.H., Walsh, J.J., Watterson, J., 1987. Displacement geometry in the volume containing a single normal fault. *AAPG Bull.* 71, 925–937.
- Bayart, E., Svetlizky, I., Fineberg, J., 2015. Fracture mechanics determine the lengths of interface ruptures that mediate frictional motion. *Nat. Phys. Lett.* <https://doi.org/10.1038/NPHYS3539>.
- Beach, A., Welbon, A.I., Brockbank, P.J., Mccallum, J.E., 1999. Reservoir damage around faults: outcrop examples from the Suez Rift. *Pet. Geosci.* 5, 109–116.
- Bense, V.F., Gleeson, T., Loveless, S.E., Bour, O., Scibek, J., 2013. Fault zone hydrogeology. *Earth Sci. Rev.* 127, 171–192.
- Ben-Zion, Y., Sammis, C., 2003. Characterization of fault zones. *Pure Appl. Geophysics* 160, 677–715.
- Bésuelle, P., Rudnicki, J.W., 2004. Localization: shear bands and compaction bands. In: Guéguen, Y., Boutéca, M. (Eds.), *Mechanics of Fluid-Saturated Rocks*. Academic Press, New York, pp. 219–321.
- Braathén, A., Tveranger, J., Fossen, H., 2009. Skar, T., Cardozo, N., Bastesen, E., Sverdrup, E., 2009. Fault facies and its application to sandstone reservoirs. *AAPG Bull.* 93, 891–917.
- Bramham, E.K., Wright, T.J., Paton, D.A., Hodgson, D.M., 2021. A new model for the growth of normal faults developed above pre-existing structures. *Geology* 49 (5), 587–591. <https://doi.org/10.1130/G48290.1>.
- Brantut, N., 2020. Dilatancy-induced fluid pressure drop during dynamic rupture: Direct experimental evidence and consequences for earthquake dynamics. *Earth Planet. Sci. Lett.* 538, 116179 <https://doi.org/10.1016/j.epsl.2020.116179>.
- Brenner, E.A., Bouchbinder, E.B., 2021. Unconventional singularities and energy balance in frictional rupture. *Nature communication* 12, 2585. Brodsky et al., 2020. The State of stress on the Fault before, during, and after a Major Earthquake. *Annu. Rev. Earth Planet. Sci.* 48, 49–74. <https://doi.org/10.1146/annurev-earth-053018-060507>.
- Brodsky, 2020. The state of stress on the fault before, during, and after a major earthquake. *Annu. Rev. Earth Planet. Sci.* 48, 49–74. <https://doi.org/10.1146/annurev-earth-053018-060507>.
- Buscarra, G., Laverack, R.T., 2014. Path dependence of the potential for compaction banding: Theoretical predictions based on a plasticity model for porous rocks. *J. Geophys. Res. Solid Earth* 119 (3), 1882–1903.
- Bönke, W., 2022. Identification and Characterization of Faults Using Deep Learning. University of Oslo. Master thesis.
- Caine, J.S., Evans, J.P., Forster, C.B., 1996. Fault zone architecture and permeability structure. *Geology* 24.
- Camanni, G., Roche, V., Childs, C., Manzocchi, T., Walsh, J., Conneally, J., Saqab, M.M., Delogkos, E., 2019. The three-dimensional geometry of relay zones within segmented normal faults. *J. Struct. Geol.* 129, 103895.
- Camanni, G., Vinci, F., Tavani, S., Ferrandino, V., Mazzoli, F., Corradetti, A., Parente, M., Lannace, A., 2021. Fracture density variations within a reservoir-scale normal fault zone: a case study from shallow-water carbonates of southern Italy. *J. Struct. Geol.* 151, 104432 <https://doi.org/10.1016/j.jsg.2021.104432>.
- Chen, J., Lu, Y., Yu, Q., Luo, X., Adeli, E., Wang, Y., Lu, L., Yuille, A.L., Zhou, Y., 2021. TransUNet: Transformers Make Strong Encoders for Medical Image Segmentation [arXiv:2102.04306v1](https://arxiv.org/abs/2102.04306v1).
- Cheng H.-D., Alexander, Cheng T., Daisy, 2005. Heritage and early history of the boundary element method. *Engineering analysis with boundary elements* 29 (3), 268–302. <https://doi.org/10.1016/j.enganabound.2004.12.001>.
- Childs, C., Manzocchi, T., Walsh, J.J., Bonson, C.G., Nicol, A., Schöpfer, M.P.J., 2009. A geometric model of fault zone and fault rock thickness variations. *J. Struct. Geol.* 31 (2), 117–127.
- Choi, J.-H., Edwards, P., Ko, K., Kim, Y.-S., 2016. Definition and classification of fault damage zones: a review and a new methodological approach. *Earth Sci. Rev.* 152, 70–87. <https://doi.org/10.1016/j.earscirev.2015.11.006>.
- Cowie, P.A., Gupta, S., Dawers, N.H., 2000. Implications of fault array evolution for synrift depocentre development: insights from a numerical fault growth model. *Basin Res.* 12 (3-4), 241–261. <https://doi.org/10.1111/j.1365-2117.2000.00126.x>.
- DeDontney, N., Templeton-Barrett, E.L., Rice, J.R., Dmowska, R., 2011. Influence of plastic deformation on bimaterial fault rupture directivity. submitted to *Journal of Geophysical Research - Solid Earth* 116 (B10). <https://doi.org/10.1029/2011JB008417>.
- Delogkos, E., Manzocchi, T., Childs, C., Camanni, G., Roche, V., 2020. The 3D structure of a normal fault from multiple outcrop observations. *J. Struct. Geol.* 136, 104009.
- Cowie, P.A., Scholz, C.H., 1992. Growth of faults by accumulation of seismic slip. *J. Geophys. Res. Solid Earth* 97, 11085–11095.
- Cruse, T.A., 1998. Boundary Element Analysis in Computational Fracture Mechanics. In: *Mechanics: Computational Mechanics*, (MCOM, volume 1), Springer. <https://doi.org/10.1007/978-94-009-1385-1>.
- Day, S.M., Dalguer, L.A., Lapusta, N., Liu, Y., 2005. Comparison of finite difference and boundary integral solutions to three-dimensional spontaneous rupture. *J. Geophys. Res.* 110, B12. <https://doi.org/10.1029/2005JB003813>.
- De Rosa, S.S., Shipton, Z.K., Lunn, R.J., Kremer, Y., Murray, T., 2018. Along-strike fault core thickness variations of a fault in poorly lithified sediments, Miri (Malaysia). *J. Struct. Geol.* 116, 189–206.
- Denolle, M.A., Shearer, P.M., 2016. New perspectives on self-similarity for shallow thrust earthquakes. *J. Geophys. Res. Solid Earth* 121, 6533–6565. <https://doi.org/10.1002/2016JB013105>.
- Di Carli, S., Francois-Holden, C., Peyrat, S., Madariaga, R., 2010. Dynamic inversion of the 2000 Tottori earthquake based on elliptical subfault approximations. *J. Geophys. Res.* 115, B12328. <https://doi.org/10.1029/2009JB006358>.
- Di Toro, G., Hirose, T., Nielsen, S., Pennacchioni, G., Shimamoto, T., 2006. Natural and Experimental Evidence of Melt Lubrication of Faults During Earthquakes. *Sci. Rep.* 311.
- Dieterich, J.H., 1979. Modeling of rock friction: 1. Experimental results and constitutive equations. *J. Geophys. Res.* 84 (B5), 2161. <https://doi.org/10.1029/JB084iB05p02161>.
- Doan, M.-L., Gary, G., 2009. Rock pulverization at high strain rate near the San Andreas fault. *Nature Geosci.* 2 (10), 709–712.
- Gabrielsen, R.H., Færseth, R.B., Jensen, L.N., Kalheim, J.E., Riis, F., 1990. Structural elements of the Norwegian Continental Shelf. Part I: The Barents Sea Region. *NPD Bull.* 6.
- Garagash, D.I., Rudnicki, J.W., 2003. Shear heating of a fluid-saturated slip-weakening dilatant fault zone 1. Limiting regimes. *J. Geophys. Res. Solid Earth* 108 (B2).
- Fisher, Q.J., Knipe, R.J., 2001. The permeability of faults within siliciclastic petroleum reservoirs of the North Sea and Norwegian Continental Shelf. *Mar. Pet. Geol.* 18, 1063–1081.
- Fung, Y.C., 1977. *A First Course in Continuum Mechanics*, 2nd edition. Prentice-Hall Inc, New Jersey.
- Giba, M., Walsh, J.J., Nicol, A., 2012. Segmentation and growth of an obliquely reactivated normal fault. *J. Struct. Geol.* 39, 253–267.
- Harris, S.D., McAllister, E., Knipe, R.J., Odling, N.E., 2003. Predicting the three-dimensional population characteristics of fault zones: a study using stochastic models. *J. Struct. Geol.* 25, 1281–1299.
- Helton, E.L., Bell, J.W., Cashman, P.H., Lazaro, M., Alm, S., 2022. Structural analysis of Southern Dixie Valley using LiDAR and low-sun-angle aerial photography, NAS Fallon geothermal exploration project, Dixie Valley, Nevada. *Transactions-Geothermal Resources Council* 35, 811–815.
- Hutchings, I., Shipway, P., 2017. *Tribology: friction and wear of engineering materials*. Butterworth-Heinemann.
- Kearse, J., Kaneko, Y., 2020. On-Fault geological fingerprint of earthquake rupture direction. *JGR Solid Earth*. <https://doi.org/10.1029/2020JB019863>.
- Jeyakumaran, M., Rudnicki, J.W., Keer, L.M., 1992. Modelling slip zones with triangular dislocation elements. *Bulletin of the Seismological Society of America* 82 (5), 2153–2169.
- Kaneko, Y., Lapusta, N., Ampuero, J.P., 2008. Spectral element modeling of spontaneous earthquake rupture on rate and state faults: Effect of velocity-strengthening friction at shallow depths. *J. Geophys. Res. Solid Earth* 113, B9. <https://doi.org/10.1029/2007JB005553>.
- Katsanos, E.I., Sextos, A.G., Manolis, G.D., 2010. Selection of earthquake ground motion records: a state-of-the-art review from a structural engineering perspective. *Soil Dyn. Earthq. Eng.* 30, 157–169.
- Kim, Y.-S., Peacock, D.C.P., Sanderson, D.J., 2004. Fault damage zones. *J. Struct. Geol.* 26, 503–517.
- Kim, Y.-S., Sanderson, D.J., 2005. The relationship between displacement and length of faults. *Earth-Sci. Rev.* 68, 317–334.
- Klinger, Y., Michel, R., King, G.C.P., 2006. Evidence for an earthquake barrier model from Mw similar to 7.8 Kokoxili (Tibet) earthquake slip-distribution. *Earth Planet. Sci. Lett.* 242, 354–364.

- Klinger, Y., Okubo, K., Vallage, A., Champenois, J., Delorme, A., Rougier, E., Lei, Z., Knight, E.E., Munjiza, A., Satrio, C., Baize, S., Langridge, R., Bhat, H., 2018. Earthquake damage patterns resolve complex rupture processes. *Geophys. Res. Lett.* <https://doi.org/10.1029/2018GL078842>.
- Kolyukhin, D., Torabi, 2012. Statistical analysis of the relationships between faults attributes. *J. Geophys. Res.* 117, B5. <https://doi.org/10.1029/2011JB008880>.
- Kolyukhin, D., Torabi, A., 2013. Power-Law Testing for Fault Attributes Distributions. *Pure and Applied Geophysics* 170 (12), 2173–2183. <https://doi.org/10.1007/s00024-013-0644-3>.
- Lapusta, N., Liu, Yi, 2009. Three-dimensional boundary integral modeling of spontaneous earthquake sequences and aseismic slip. *J. Geophys. Res. Solid Earth* 114, B9. <https://doi.org/10.1029/2008JB005934>.
- Lay, T., Wallace, T.C., 1995. *Modern global seismology*. Academic Press, California, 522 pages.
- Liu, Y., 2009. Three-Dimensional Elastodynamic Modeling of Frictional Sliding with Application to Interseismic Deformation. Dissertation (Ph.D.), California Institute of Technology. <https://doi.org/10.7907/JWCV-8V74>.
- Loveless, S., Pluymaekers, M., Lagrou, D., Boever, E., Doornenbal, H., Laenen, B., 2014. Mapping the Geothermal potential of Fault zones in the Belgium-Netherlands Border Region. *Energy Proc.* 59, 351–358.
- Oikonomou, D., Larsen, E., Alaei, B., Stefos, G., and Purves, S., 2019, EarthNET a native cloud web based solution for next generation subsurface workflows, [ba1] 81st EAGE Conference and Exhibition 2019 Workshop Programme, p.1 – 4.
- Okubo, K., Bhat, H.S., Rougier, E., Marty, S., Scubnel, A., Lei, Z., Knight, E.E., Klinger, Y., 2019. Dynamics, radiation, and overall energy budget of earthquake rupture with coseismic off-fault damage. *JGR Solid Earth* 124, 11771–11801.
- Madariaga, R., Ruiz, S., 2016. Earthquake dynamics on circular faults, a review 1970–2015. *J. Seismol.* <https://doi.org/10.1007/s10950-016-9590-8>.
- Manighetti, I., Campillo, M., Bouley, S., Cotton, F., 2007. Earthquake scaling, fault segmentation, and structural maturity. *Earth Planet. Sci. Lett.* 253 (3), 429–438.
- Manighetti, I., Campillo, M., Sammis, C., Mai, P.M., King, G., 2005. Evidence for self-similar, triangular slip distributions on earthquakes: Implications for earthquake and fault mechanics. *J. Geophys. Res.* 110, B05302.
- Marchal, D., Guiraud, M., Rives, T., 2003. Geometric and morphologic evolution of normal fault planes and traces from 2D to 4D data. *J. Struct. Geol.* 25, 135–158.
- Marone, C., Raleigh, C.B., Scholz, C.H., 1990. Frictional behavior and constitutive modeling of simulated fault gouge. *J. Geophys. Res.* 95, B5. <https://doi.org/10.1029/JB095IB05p07007>.
- Marple, R.T., Hurd, 2020. Interpretation of lineaments and faults near Summerville, South Carolina, USA, using LiDAR data: implications for the cause of the 1886 Charleston, South Carolina, earthquake. *Atlantic Geol.* 56, 73–95. <https://doi.org/10.4138/atgeol.2020.003>.
- Marrett, R., Allmendinger, R.W., 1991. Estimates of strain due to brittle faulting: sampling of fault populations. *J. Struct. Geol.* 13 (6), 735–738.
- Marone, C., Raleigh, C.B., Scholz, C.H., 1990. Frictional Behavior and Constitutive Modeling of simulated Fault Gouge. *J. Geophys. Res.* 95 (B5), 7007–7025.
- Martel, S.J., Pollard, D.D., 1989. Mechanics of slip and fracture along small faults and simple strike-slip fault zones in Granitic Rock. *J. Geophys. Res.* 94 (B7), 9417–9942.
- McBeck, J., Ben-Zion, Y., Renard, F., 2022. Volumetric and shear strain localization throughout triaxial compression experiments on rocks. *Tectonophysics* 822, 229181.
- Moës, N., Dolbow, J., Belytschko, T., 1999. A finite element method for crack growth without remeshing. *Int. J. Numer. Methods Eng.* 46 (1), 131–150.
- Moore, D.E., Lockner, D.A., 1995. The role of microcracking in shear-fracture propagation in granite. *J. Struct. Geol.* 17 (1), 95–114.
- Michie, E.A.H., Alaei, B., Braathen, A., 2021. Assessing the accuracy of fault interpretation using machine-learning techniques when risking faults for CO2 storage site assessment. *Interpretation* 10, 1.
- Nicol, A., Watterson, J., Walsh, J.J., Childs, C., 1996. The shapes, major axis orientations and displacement patterns of fault surfaces. *J. Struct. Geol.* 18 (2/3), 235–248.
- Palmer, A.C., Rice, J.R., 1973. The growth of slip surfaces in the progressive failure of overconsolidated clay. *Proc. R. Soc. Lond. Ser. A* 332, 527–548.
- Perrin, C., Manighetti, I., Ampuero, J.-P., Cappa, F., Gaudemer, Y., 2015. Location of largest earthquake slip and fast rupture controlled by along-strike change in fault structural maturity due to fault growth. *JGR Solid Earth.* <https://doi.org/10.1002/2015JB012671>.
- Perrin, C., Manighetti, I., Gaudemer, Y., 2016. Off-fault tips play networks: a genetic and generic property of faults indicative of their long-term propagation. *Tectonophysics* 348, 52–60.
- Petricca, P., Bignami, C., Daglioni, C., 2021. The epicentral fingerprint of earthquakes marks the coseismically activated crustal volume. *Earth Sci. Rev.* 218, 103667 <https://doi.org/10.1016/j.earscirev.2021.103667>.
- Preuss, S., Ampuero, J.P., Gerya, T., van Dinther, Y., et al., 2020. Characteristics of earthquake ruptures and dynamic off-fault deformation on propagating faults. *Solid Earth* 11, 1333–1360. <https://doi.org/10.5194/se-11-1333-2020>.
- Rice, R. 1968. Mathematical analysis in the mechanics of fracture. See Liebowitz 1968 II: 191–311.
- Roche, V., Camanni, G., Childs, C., Manocchi, T., Walsh, J., Conneally, J., Saqab, M.M., Delogkos, 2021. Variability in the three-dimensional geometry of segmented normal fault surfaces. *Earth Sci. Rev.* 216, 103523.
- Rohmer, J., Nguyen, K., Torabi, A., 2015. Off-fault shear failure potential enhanced by high stiff/low permeable damage zone during fluid injection in porous reservoirs. *Geophys. J. Int.* 202, 1566–1580.
- Ronneberger, O., Fisher, P., Brox, T., 2015. U-Net: Convolutional Networks for Biomedical Image Segmentation. Part of the lecture notes in computer science book series (LNIP, V. 9351), arXiv:1505.04597v1.
- Rotevatn, A., Jackson, C.A.-L., Tvedt, A.B.M., Bell, R.E., 2019. How do normal faults grow? *J. Struct. Geol.* 125 <https://doi.org/10.1016/j.jsg.2018.08.005>.
- Rudnicki, 1980. Fracture mechanics applied to Earth's crust. *Ann. Rev. Earth Planet. Sci.* 8, 489–525.
- Romanet, P., Bhat, H.S., Jolivet, R., Madariaga, R., 2018. Fast and slow events emerge due to fault geometrical complexity. *Geophys. Res. Lett.* 45, 4809–4819.
- Rudnicki, J.W., Rice, J.R., 1975. Conditions for the localization of deformation in pressure-sensitive dilatant materials. *J. Mech. Phys. Solids* 23 (6), 371–394.
- Ruina, A., 1983. Slip instability and state variable friction laws. *J. Geophys. Res. Solid Earth* 88 (B12), 10359–10370. <https://doi.org/10.1029/JB088B12p10359>.
- Savage, H.M., Brodsky, E.E., 2011. Collateral damage: Evolution with displacement of fracture distribution and secondary fault strands in fault damage zones. *J. Geophys. Res. Solid Earth* 116.
- Scholz, C.H., Cowie, P.A., 1990. Determination of total strain from faulting using slip measurements. *Nature* 346, 837–839.
- Shipton, Z.K., Soden, A., Kirkpatrick, J.D., Bright, A.M., 2006. How thick is a fault? Fault displacement thickness scaling revisited. In: Abercrombie, R. (Ed.), *Earthquakes: Radiated Energy and the Physics of Faulting*, AGU Geophysical Monograph Series, 170, pp. 193–198.
- Skurtveit, E., Torabi, A., Gabrielsen, R.H., Zoback, M., 2013. Experimental investigation of deformation mechanisms during shear enhanced compaction in poorly lithified sandstone and sand. *J. Geophys. Res.* 118, 4083–4100.
- Schultz, R.A., Fossen, H., 2002. Displacement-length scaling in three dimensions: the importance of aspect ratio and application to deformation bands. *J. Structural Geol.* 24, 1389–1411.
- Shahin, G., Torabi, A., Rudnicki, J., Buscarnera, G., 2021. The role of stratigraphy and loading history in generating complex compaction bands in idealized field-scale settings. *J. Geophys. Res. Solid Earth* 126 (2), e2020JB020452.
- Shahin, G., Viggiani, G., Buscarnera, G., 2020. Simulating spatial heterogeneity through a CT-FE mapping scheme discloses boundary effects on emerging compaction bands. *Int. J. Solids Struct.* 206, 247–261.
- Scholz, C.H., 2007. Mechanics of faulting. *Annu. Rev. Earth Planet. Sci.* <https://doi.org/10.1146/annurev.earth.17.1.309>.
- Scholz, C.H., 2019. *The mechanics of earthquakes and faulting*. Cambridge University Press.
- Tibaldi, A., Corti, N., De Beni, E., Bonali, F.L., Falsaperla, S., Langer, H., Neri, M., Cantarero, M., Reitano, D., Fallati, L., 2021. Mapping and evaluating kinematics and the stress and strain field at active faults and fissures: a comparison between field and drone data at the NE rift, Mt Etna (Italy). *EGU Solid Earth* 12, 801–816. <https://doi.org/10.5194/se-12-801-2021>.
- Tan, M., Le, Q.V., 2019. EfficientNet: Rethinking Model Scaling for Convolutional Neural Networks. *PMLR*, Long Beach, California, 97.
- Templeton, E.L., Rice, J.R., 2008. Off-fault plasticity and earthquake rupture dynamics: Dry materials or neglect of fluid pressure changes. *J. Geophys. Res.* 113, B9.
- Torabi, A., Alaei, B., 2022. Fault characterization challenges and advances in deep learning, keynote talk. In: *Sixt EAGE Fault and Top Seal Conference*, Vienna, 26–28 September.
- Torabi, A., Alaei, B., Libak, A., 2019a. Normal fault 3D geometry and displacement revisited; Insights from faults in the Norwegian Barents Sea. *Mar. Pet. Geol.* 99, 135–155.
- Torabi, A., Johannessen, M.U., Ellingsen, T.S.S., 2019b. Fault core-Insights from siliciclastic and carbonate rocks. *Geofluids* 2019. <https://doi.org/10.1155/2019/2918673>, 24 Article ID 2918673.
- Torabi, A., Berg, S.S., 2011. Scaling of fault attributes, a review. *Mar. Pet. Geol.* 28 (8), 1444–1460.
- Torabi, A., Braathen, A., Cuisiat, F., Fossen, H., 2007. Shear zones in porous sand: Insights from ring-shear experiments and naturally deformed sandstones. *Tectonophysics* 437, 37–50.
- Torabi, A., Ellingsen, T.S.S., Johannessen, M., Alaei, B., Rotevatn, A., Chiarella, D., 2020. Fault zone architecture and its scaling laws: where does the damage zone start and stop? In: Ogilvie, S.R., Dee, S.J., Wilson, R.W., Bailey, W.R. (Eds.), *Integrated Fault Seal Analysis*, 496. Geological Society, London, pp. 99–124. Special Publications.
- Treffelsen, T., Henk, A., 2020. Faults as Volumetric Weak Zones in Reservoir-Scale Hydro-Mechanical Finite Element Models—A Comparison Based on Grid Geometry, Mesh Resolution and Fault Dip. *Engines* 13, 2673.
- Ulrich, T., Gabriel, A.A., Madden, E., 2022. Stress, rigidity and sediment strength control megathrust earthquake and tsunami dynamics. *Nat. Geosci.* 15, 67–73.
- Vallage, A., Klinger, Y., Lacassin, R., Delorme, A., Pierrot-Deseilligny, M., 2016. Geological structures control on earthquake ruptures: the Mw7.7, 2013, Balochistan earthquake, Pakistan. *Geophys. Res. Lett.* 43 <https://doi.org/10.1017/9781316681473>.
- Vermilye, J.M., Scholz, C.H., 1998. A microstructural view of fault growth. *J. Geophys. Res.* 103 (B6), 12223–12237.
- Walsh, J.J., Watterson, J., 1988. Analysis of the relationship between displacements and dimensions of faults. *J. Struct. Geol.* 10, 238–347.
- Walsh, J.J., Nicol, A., Childs, C., 2002. An alternative model for the growth of faults. *J. Struct. Geol.* 24 (11), 1669–1675.
- Viesca, R., Garagash, D.I., 2018. Numerical methods for coupled fracture problems. *Journal of the mechanics and physics of solids* 113, 13–34. <https://doi.org/10.1016/j.jmps.2018.01.008>.
- Viesca, R., Templeton, E.L., Rice, J.R., 2008. Off-fault plasticity and earthquake rupture dynamics: 2. Effects of fluid saturation. *Solid Earth* 113, B9. <https://doi.org/10.1029/2007JB005530>.
- Walsh, J.J., Bailey, W.R., Childs, C., Nicol, A., Bonson, C.G., 2003. Formation of segmented normal faults: a 3-D perspective. *J. Struct. Geol.* 25, 1251–1262.

- Wang, H., Jiang, Y., Xue, S., Mao, L., Lin, Z., Deng, D., Zhang, D., 2016. Influence of fault slip on mining-induced pressure and optimization of roadway support design in fault-influenced zone. *J. Rock Mech. Geotech. Eng.* 8, 660–671.
- Wechsler, N., Ben-Zion, Y., Christofferson, S., 2010. Evolving geometrical heterogeneities of fault trace data. *Geophys. J. Int.* 182, 551–567.
- Wu, M., Rudnicki, J.W., Kuo, C.H., Keer, L.M., 1990. Surface deformation and energy release rates for constant stress drop slip zones in an elastic half-space. *J. Geophys. Res. Solid Earth* 96 (B10), 16509–16524. <https://doi.org/10.1029/91JB01043>.
- Wu, X., Yan, S., Bi, Z., Zhang, S., Si, H., 2021. Deep learning for multidimensional seismic impedance inversion. *Geophysics* 86, 5.
- Yang, D., Cai, Y., Hu, G., Yao, X., 2020. Seismic fault detection based on 3D Unet++ model. In: Society of Exploration Geophysicists, SEG International Exposition and 90th Annual Meeting. <https://doi.org/10.1190/segam2020-3426516.1>.
- Ybanez, R.L., Ybanez, A.A.A., Lagmay, A.M.F.A., Aurelio, A.A., 2021. Imaging ground surface deformations in post-disaster settings via small UAVs. *Geosci. Lett.* 8, 23. <https://doi.org/10.1186/s40562-021-00194-8>.
- Zaccagnino, D., Telesca, L., Doglioni, C., 2022. Scaling properties of seismicity and faulting. *Earth Planet. Sci. Lett.* 584, 117511 <https://doi.org/10.1016/j.epsl.2022.117511>.